8. The role of pDCs in immunity to influenza virus infection

8.1. Introduction

Respiratory infections such as those caused by influenza virus A constitute a major health problem and can result in worldwide pandemics. A combination of innate and adaptive immune mechanisms are required to resolve the infection. A key function in bridging the two branches of the immune system has been ascribed to DCs. PDCs are uniquely equipped to recognize viral nucleic acids through the expression of TLR7 and TLR9 [43, 44]. It has become clear that pDCs are specialized to rapidly produce large amounts of type I interferons after stimulation with influenza virus. In the defense against viral infections, type I interferons are believed to play an important role [212].

In the steady-state, pDCs have been shown to reside within the lungs, most likely to sense viral intruders. Data presented in the first chapter showed that pDCs can secrete a variety of chemokines, which could attract other leukocytes, especially NK cells and T cells, into the lung compartment during infection [120, 123]. In addition, several studies suggested that pDCs may be involved in antigen presentation regulating T cell activation in viral infections. For that purpose, they may migrate from the lungs to draining mediastinal LNs (see chapter 2 and [39, 129]). pDCs activated by certain viruses have been shown to induce T cell proliferation [96, 104, 183] and differentiation into Th1 and/or IFN-γ-/IL-10-producing cells [101, 105, 114], although others have demonstrated that pDCs are unable to present antigen to naïve T cells [109, 110]. In chapter one, we have determined that PR8 virus-activated pDCs are relatively poor inducers of $CD8^+$ T cell proliferation. Others have shown that type I interferon produced by pDCs could act directly on T cells allowing for clonal expansion [213, 214], and could induce maturation and antigen presenting function of mDCs [89, 174, 182]. Finally, in lung-draining lymph nodes, pDCs may interact with B cells as it has been shown that pDC-derived IFN-α functions together with IL-6 in promoting B cell maturation and antibody production [97].

Recently, two studies independently showed that depletion of pDCs in a model of respiratory syncytial virus infection resulted in promoted pulmonary pathology and decreased viral clearance [172, 173]. However, most of the strategies of pDC depletion involve antibodies such as Ly6C/G, 120G8 and mPDCA-1 that potentially decrease other important cell types in the immune response, which express these markers during infection. To circumvent this problem, we made use of a recently described novel mouse strain, Ikaros$^{L/L}$, which lack peripheral pDCs, but harbor normal numbers of DCs [49, 167]. The goal of our experiments was to elucidate the role of pDCs in response to influenza virus infection.

8.2. Results

8.2.1. pDC numbers increase in lungs and airways of influenza PR8-infected mice

First, we determined the behavior of pDCs during influenza virus infections. We infected anesthetized DPE^{GFP} mice intranasally with influenza virus A/PR/8/34. Under these conditions, mice develop an infection of the total respiratory tract. Similar to WT animals, DPE^{GFP} mice started to loose weight around day 4 post infection (p.i.), with a peak around day 10 p.i., at which time point mice had lost up to 30% of their starting weight (Figure 32A). During recovery, their weight returned to the original starting level within 15 days post infection. To investigate the numbers of pDCs in various organs following infection, we identified pDCs based on GFP expression and staining with CD45R/B220 or mPDCA-1. Whereas pDCs were absent in the bronchioalveolar lavage fluid of naïve, uninfected mice, we observed a robust influx of pDCs into the airways starting as early as 2-3 days p.i., and peaking around day 7 p.i. (Figure 32C). A 5-fold increase in pDC numbers was sustained in the parenchyma up to 15 days p.i., from where it declined to a 2-fold increase at 3 weeks post infection (Figure 32B). In contrast, pDC numbers in spleens remained constant over the period of the infection (Figure 32D). In lung-draining mediastinal lymph nodes (medLN), we found 10-fold lower pDC numbers compared to conventional $CD11c^{hi}$ cells (Figure 32E-F). Moreover, $CD11c^{hi}$ cells accumulated at day 3 p.i. (6-8-fold increase over control), consistent with the paradigm of influx of mDC accumulation (Figure 32F). On the other hand, the influx of pDCs was not observed until day 5 p.i. (Figure 32E). Thus, while pDCs were recruited into the lungs and airways early during the anti-influenza response, pDCs have a delayed influx into draining LN as compared to mDCs during infection.

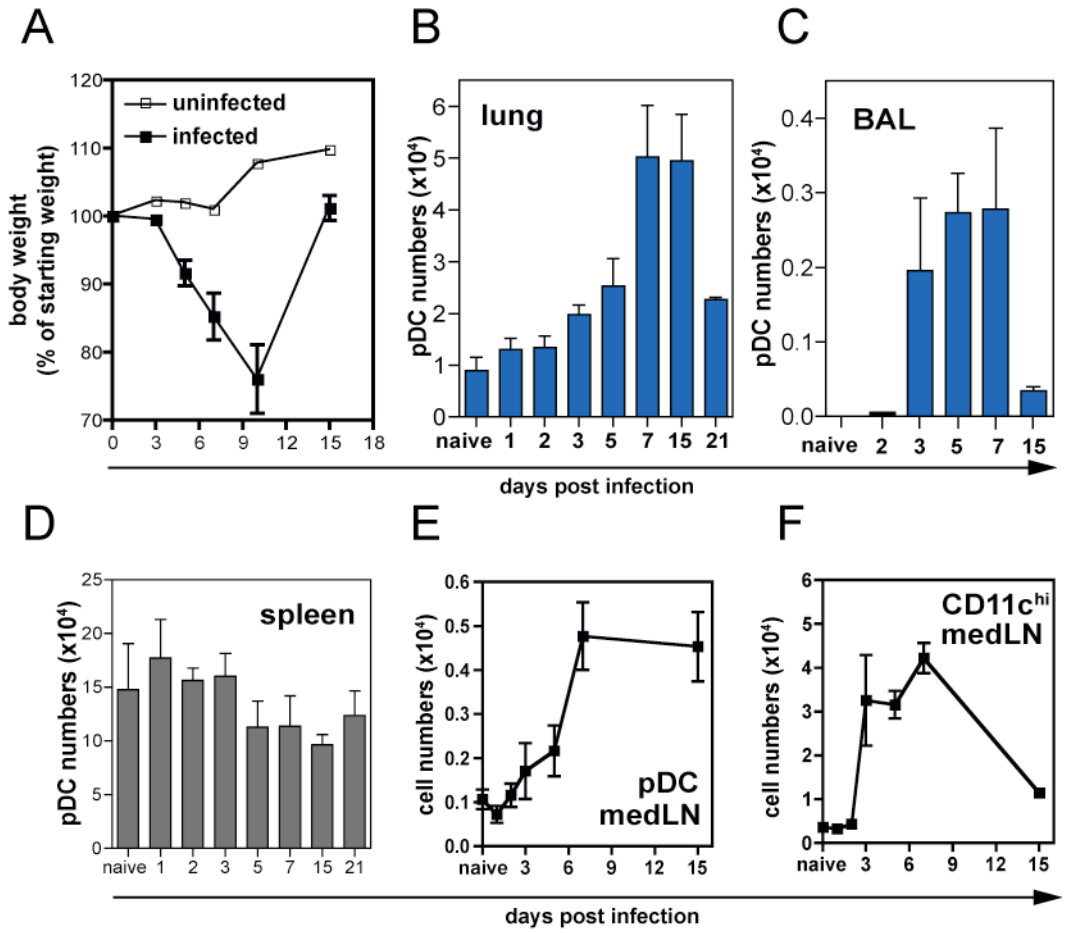

Figure 32: pDC numbers increase in lungs and airways during influenza PR8 virus infection.

DPE^{GFP} mice were infected intranasally with influenza virus A/PR/8/34. (**A**) Weight curves of uninfected (open squares) and PR8 infected DPE^{GFP} mice (closed squares) (n=2-5 mice per time point). (**B-F**) At different time points following infections with PR8 virus, single cell suspensions from lungs (**B**), bronchoalveolar space (BAL) (**C**), spleen (**D**) and mediastinal LN (**E-F**) were analyzed by flow cytometry for the presence of GFP^{hi} B220^{+} pDCs (**B-E**) or CD11c^{hi} mDCs (**F**).

When we assessed the maturation status of GFP^{hi} B220^{+} pDCs in the lungs of influenza-infected DPE^{GFP} mice, these cells had an activated phenotype as revealed by the expression of CD86 compared to pDCs in lungs of non-infected controls (Figure 33). CD40 expression,

however, remained low on pDCs from infected mice consistent with the results of cultured pDCs (chapter one). Over the course of the infection, pDCs in spleen remained CD86^{low} (data not shown).

Figure 33: Maturation status of pDCs in lungs following influenza PR/8 virus infection.

A single cell suspension from lungs of a DPE^{GFP} mouse was stained for GFP^{hi} B220^{+} pDCs and presented as a contour plot (left). (Right graph) Histograms are gated on GFP^{hi} B220^{+} cells and depict staining with a control IgG antibody (open) and CD86 expression in lungs of a naïve (grey) or infected (black) mouse (day 7 p.i.).

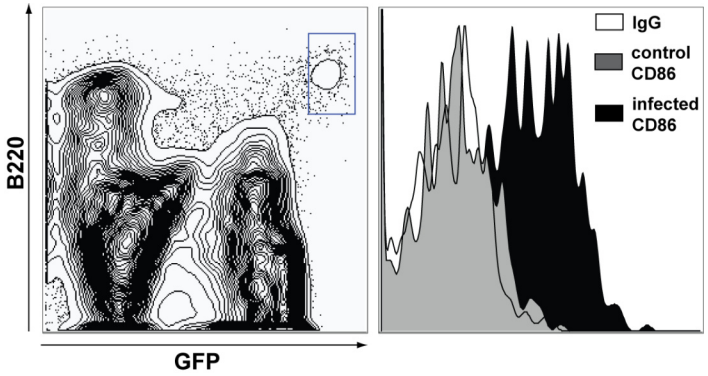

8.2.2. Ikaros$^{L/L}$ mice lack peripheral pDCs

In order to investigate the role of pDCs in immunity to influenza infection, we obtained Ikaros$^{L/L}$ mice that lack peripheral pDCs. This mouse strain was generated by inserting a β-galactosidase reporter gene into the 5' part of the Ikaros exon 3 locus through homologous recombination in embryonal stem cells [167]. In spleen and lymph nodes of Ikaros$^{L/L}$ mice, pDCs were reported to be absent [49]. Due to the mutation in the Ikaros locus, pDCs were blocked in their differentiation in the bone marrow (BM). In comparison to pDCs in the BM of wild-type mice, pDCs from Ikaros$^{L/L}$ mice express some markers characteristic for pDCs, such as the 120G8 antigen. However, they express only low levels of CD11c, are mainly Ly49Q^{-} and lack B220 expression. Most importantly, IFN-α production in response to viral activation was impaired, indicating that those pDCs are not functional [49].

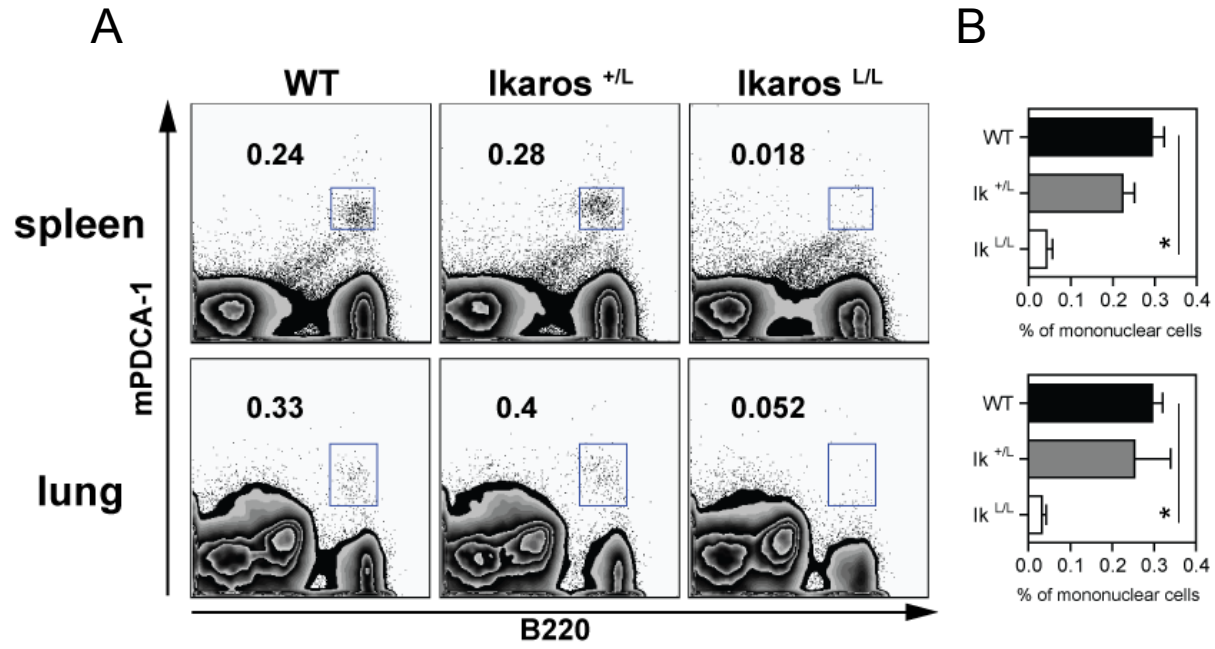

Figure 34: pDCs are mostly absent in spleens and lungs of Ikaros$^{L/L}$ mice.

(**A**) Single cell suspensions of wild-type (WT), Ikaros$^{+/L}$ and Ikaros$^{L/L}$ mice were analyzed for the presence of B220^{+} PDCA^{+} pDCs. Numbers in FACS plots represent percentage of total cells. (**B**) The percentage of pDCs in spleens (top) and lungs (bottom) of WT, Ikaros$^{+/L}$ and Ikaros$^{L/L}$ mice was graphed (n=3 mice). Statistical significance between the three groups was calculated using one-way ANOVA with Bonferroni's correction.

To confirm that Ikaros$^{L/L}$ mice also have a loss in pDCs in organs relevant for the influenza infection model, we harvested spleens and lungs of Ikaros$^{L/L}$, heterozygous Ikaros$^{+/L}$, and WT littermates and stained single cell suspensions with αB220 and mPDCA-1. As indicated in Figure 34, WT animals had significantly higher percentages (6-13-fold higher) of pDCs in lungs and spleen compared Ikaros$^{L/L}$ mice. A significant reduction of pDCs in other organs such as lymph nodes of Ikaros$^{L/L}$ mice was also confirmed (data not shown). Heterozygous mice harbored intermediate numbers of pDCs.

Collectively, we concluded that Ikaros$^{L/L}$ mice have a lack of pDCs in peripheral organs and thus present a powerful tool to study *in vivo* immune responses to influenza infection in the absence of pDCs.

8.2.3. Normal maturation of mDC but impaired IFN-α production of splenic cells from Ikaros$^{L/L}$ mice following stimulation with PR8 virus *in vitro*

Next, we tested whether the absence of pDCs in Ikaros$^{L/L}$ mice led to impaired IFN-α production upon stimulation with PR8 virus. We harvested splenocytes from wild-type, Ikaros$^{+/L}$ and Ikaros$^{L/L}$ mice and cultured them overnight with and without PR8 virus. In line with previous results, we detected IFN-α in the supernatants of WT-splenocytes, but not splenocytes of Ikaros$^{L/L}$ mice that had been cultured with PR8 virus (Figure 35). The amount of IFN-α from Ikaros$^{+/L}$ mice was somewhat variable.

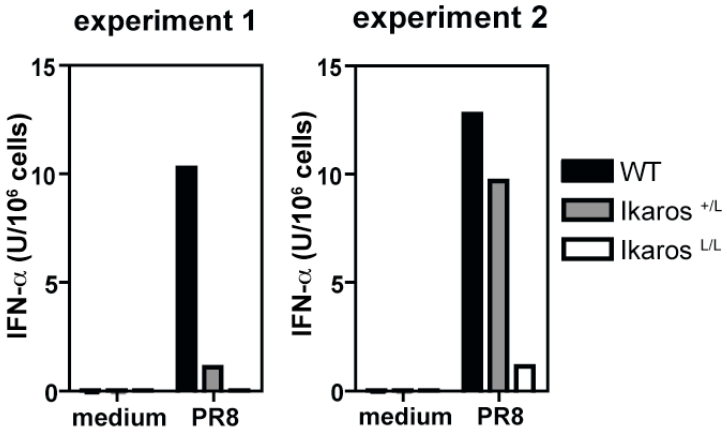

Figure 35: Impaired IFN-α production of splenocytes from Ikaros$^{L/L}$ mice.

Single cell suspensions from spleens of WT, Ikaros$^{+/L}$ and Ikaros$^{L/L}$ mice were cultured overnight in medium with or without 1000 HAU/ml purified, UV-inactivated PR8 virus. Supernatants were tested in an ELISA for IFN-α.

Of note, the percentage of CD11c^{hi} mDCs was comparable in the spleen of WT and Ikaros$^{L/L}$ mice (Figure 36A). Splenocytes from Ikaros$^{L/L}$ mice harbored slightly lower B cell numbers directly *ex vivo* (data not shown) and after culture in medium or with PR8 virus

(WT: 48% vs. $Ik^{L/L}$: 38%) (see Figure 36A). Upon stimulation with PR8 virus, mDCs and B cells of $Ikaros^{L/L}$ mice upregulated the costimulatory molecules CD40 and CD86, indicating that mDC and B cell maturation proceeded normally (Figure 36B and C). In addition, activation of mDCs with LPS induced their normal activation (data not shown).

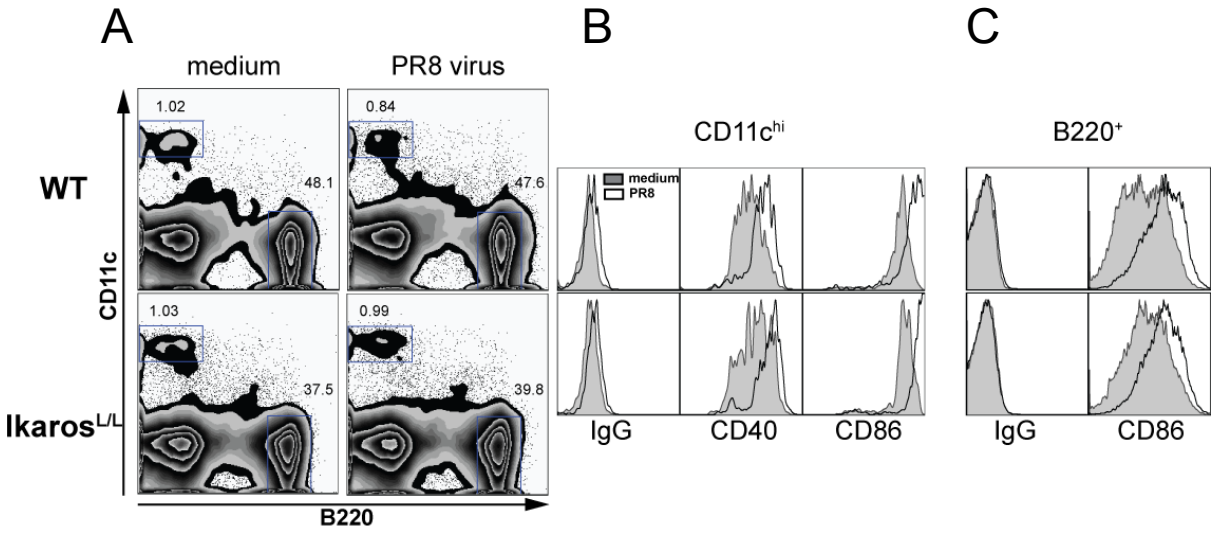

Figure 36: Maturation of splenic mDC and B cells is normal following activation with PR8 virus *in vitro*.

(**A-C**) Splenocytes from WT (top) and $Ikaros^{L/L}$ (bottom) mice were cultured overnight in medium with or without PR8 virus. (**A**) The percentage of $CD11c^{hi}$ (mDCs) and $B220^{+}$ $CD11c^{-}$ B cells was determined by flow cytometry and results are displayed in Zebra plots. Histograms of the expression of costimulatory molecules CD40, CD86 and staining with an isotype control antibody are shown for mDCs (**B**) and B cells (**C**) within splenocytes cultured in medium without (grey) or with (open histogram) PR8 virus.

8.2.4. Ikaros$^{L/L}$ mice mount a normal immune response to influenza virus infection

In order to determine whether the absence of pDCs during influenza infection affects the course of disease, WT and Ikaros$^{L/L}$ mice were infected intranasally with a sublethal dose of influenza PR8 virus. Both groups developed a comparable progression of infection as indicated by the weight loss curves (Figure 37A). Also, Ikaros$^{L/L}$ mice did not show increased mortality. Compared to wild-type mice, Ikaros$^{L/L}$ mice gained weight slightly more slowly. These data suggest that the overall course of influenza virus infection, including the disease recovery, was normal in the absence of pDCs.

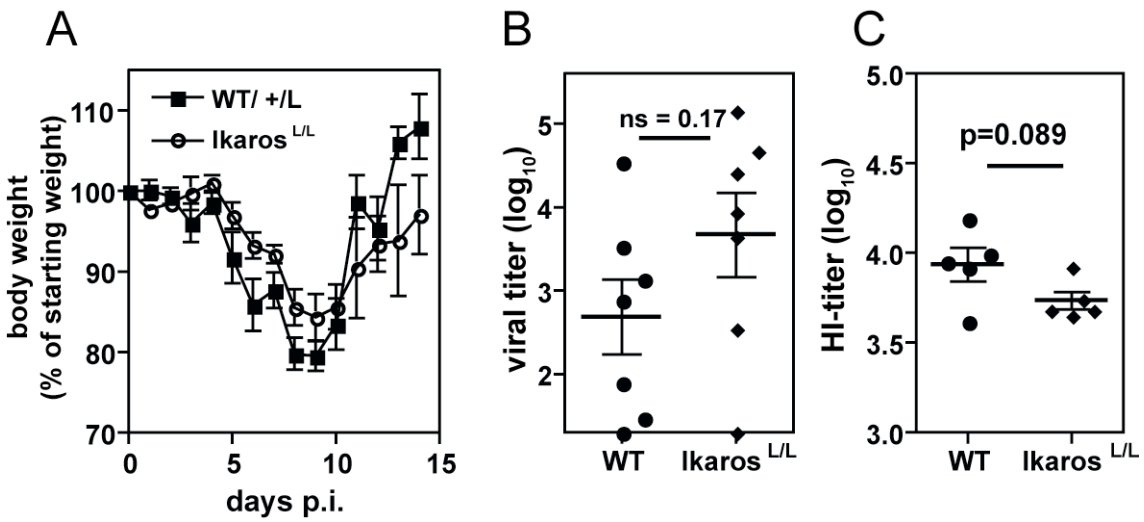

Figure 37: Course of influenza disease in Ikaros$^{L/L}$ mice following PR8 virus infection.

Wild-type (or in some cases Ikaros$^{+/L}$ mice) and Ikaros$^{L/L}$ mice were infected intranasally with a sublethal dose of influenza A/PR/8/34 virus. (**A**) Body weight of infected mice (n=3-15) was measured over time. (**B**) Lungs of WT and Ikaros$^{L/L}$ mice were harvested at day 8 p.i. and viral titers determined in MDCK cell cultures and hemagglutination assays. (**C**) In a hemagglutination inhibition (HI) assay, sera of WT and Ikaros$^{L/L}$ mice at day 39 p.i. were analyzed for PR8 virus neutralizing antibody titers.

For determination of viral titers, lungs of infected animals were harvested at day 8 p.i., and supernatants cultured on MDCK cells. There was a trend for higher viral titers in the lungs of Ikaros$^{L/L}$ mice, however, the difference was not statistically significant (Figure 37B). One day later, infectious virus in lungs of either wild-type or Ikaros$^{L/L}$ mice was undetectable with this method (data not shown), indicating that virus was cleared in the absence of pDCs.

It has previously been shown that virus-stimulated pDCs contribute to B cell differentiation into plasma cells, and that depletion of pDCs from human PBL abrogated production of anti-influenza antibodies [97]. Thus, we assessed whether Ikaros$^{L/L}$ mice have a defect in the production of virus-neutralizing antibodies. When we analyzing the serum from animals at day 39 p.i., we found that Ikaros$^{L/L}$ mice had comparable levels of neutralizing antibody titers (Figure 37C), indicating normal B cell responses.

8.2.5. B220$^-$ CD11c$^-$ mPDCA-1$^+$ pDC precursors in the bone marrow of Ikaros$^{L/L}$ mice do not differentiate into conventional pDCs after Flt-3L treatment and influenza virus infection *in vivo*

In light of these unexpected results, we investigated whether pDCs could be detected in Ikaros$^{L/L}$ mice during influenza infection. As mentioned above, Allman et al. described a pDC precursor present in the bone marrow of Ikaros$^{L/L}$ mice [49]. Hence, we tested the possibility that these precursors may have exited the BM during an immune response, and differentiated into functional pDCs.

Phenotypically, the pDC precursors from Ikaros$^{L/L}$ BM are B220$^-$ and CD11c$^-$ as compared to B220$^+$ CD11c^{int} Ly6C$^+$ 120G8$^+$ pDCs in wild-type mice. Using a gating strategy that eliminates lineage (lin) positive (CD3$^+$ CD19$^+$ Nk1.1$^+$ CD11b$^+$) cells and includes mPDCA-1 as a marker for pDCs, we found mPDCA-1$^+$ in the BM of Ikaros$^{L/L}$ mice, albeit at a slightly decreased frequency as compared to WT BM (Figure 38A). mPDCA-1$^+$ lin$^-$ cells

from Ikaros$^{L/L}$ BM were B220^{-} CD11c^{-} in contrast to positive staining for B220 and CD11c in WT mice. However, the cells expressed equal levels of CD4 and Ly6C/G (Figure 38B, and data not shown). Next, we analyzed whether these cells could produce IFN-α. In agreement with published results, we found that production of IFN-α by PR8 virus-activated BM cells from Ikaros$^{L/L}$ mice was greatly diminished as compared to the IFN-α levels produced by BM cells from wild-type mice (Figure 38C), indicating that the mPDCA-1^{+} lin^{-} pDC-precursors had a defect in responding to viral stimulation. Together, it seems likely that the mPDCA-1^{+} lin^{-} cells in Ikaros$^{L/L}$ mice are dysfunctional.

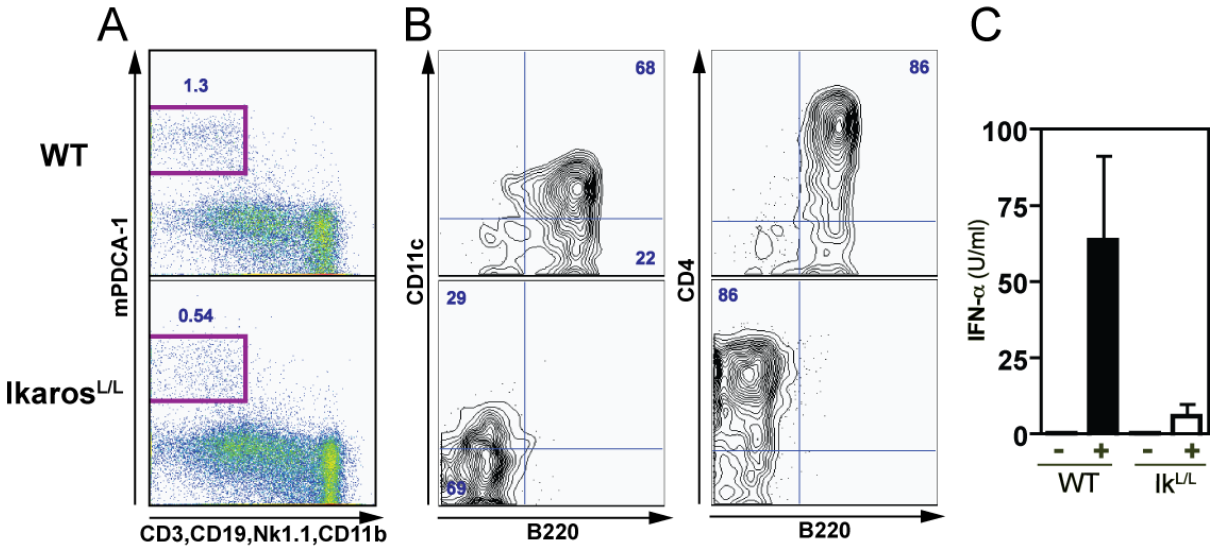

Figure 38: Bone marrow of Ikaros$^{L/L}$ mice harbors mPDCA-1^{+} pDC precursors that are unable to produce high levels of IFN-α.

(**A**) Single cell suspensions from bone marrow of WT (top panels) and Ikaros$^{L/L}$ mice (bottom panels) were stained for lineage (lin) markers (CD3, CD19, Nk1.1, CD11b) and mPDCA-1. Numbers depict the percentage of lin^{-} mPDCA-1^{+} cells within all live cells. One representative staining out of 2 independent experiments is shown. (**B**) The expression of B220, CD11c and CD4 on lin^{-} mPDCA-1^{+} cells is shown. Numbers represent the percentage of cells in the respective quadrants. (**C**) BM cells from WT and Ikaros$^{L/L}$ mice were cultured overnight without (-) or with (+) 1000 HAU/ml purified, UV-treated influenza virus PR8. Supernatants were tested for IFN-α by ELISA. Results are shown as mean ± SEM for n=3 mice per group.

We next determined the fate of pDC precursors in Ikaros$^{L/L}$ mice following treatment with Flt-3L *in vivo*. Allman et al. has previously shown that the pDC precursors derived from Ikaros$^{L/L}$ BM express normal levels of the receptor for Flt-3L, and that the cells expanded after Flt-3L treatment *in vitro* [49]. We implanted B16-Flt-3L melanoma cells into WT and Ikaros$^{L/L}$ mice and analyzed the percentage of PDCA-1$^+$ cells in various organs after 13 days. Both mouse strains developed equally sized tumors (data not shown). Although the total cell numbers of spleens and lymph nodes were comparable between the strains, mPDCA-1$^+$ cells in Ikaros$^{L/L}$ mice had expanded much less as compared to WT mice (Figure 39A and B). Moreover, the analysis of their phenotype revealed that these cells were unable to differentiate into *bona fide* pDCs upon Flt-3L treatment (see Figure 39C).

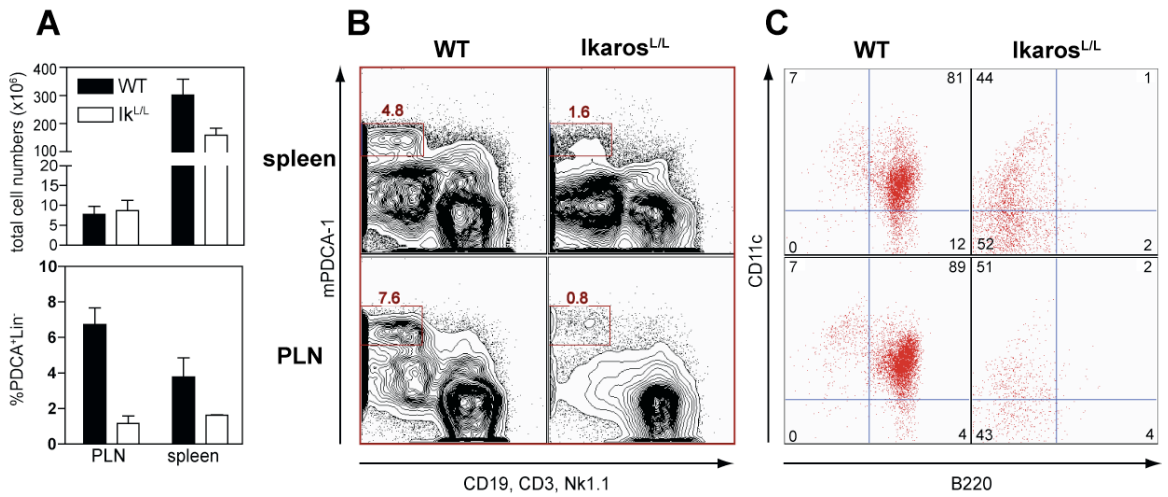

Figure 39: Impaired expansion of pDC precursors of Ikaros$^{L/L}$ mice in response to Flt-3L *in vivo*.

WT and Ikaros$^{L/L}$ mice were implanted subcutaneously with B16-Flt-3L cells. 13 days later, spleens and PLN were harvested and stained for mPDCA-1 and lineage markers (CD19, CD3 and Nk1.1.). (**A**) Total cell numbers (top) and percentage of mPDCA-1$^+$ lin$^-$ cells (bottom) were enumerated based on the gates depicted in the flow cytometry staining shown in (**B**). (**C**) Cells in the mPDCA-1$^+$ lin$^-$ gate shown in (**B**) were analyzed for the expression of B220 and CD11c.

In order to exclude that influenza infection induces the egress of pDC precursors from the BM in Ikaros$^{L/L}$ mice spleens and lungs from infected wild-type and Ikaros$^{L/L}$ mice were harvested stained with anti-B220 and mPDCA-1. At day 10 p.i. as well as at other time points during infection (Figure 40 and data not shown), no B220^{+} PDCA-1^{+} cells were found in spleens, lungs and BAL of Ikaros$^{L/L}$ mice. This suggests that the pDC precursors detected in the BM in Ikaros$^{L/L}$ mice were unable to differentiate into mature B220^{+} PDCA-1^{+} in the periphery during infection. We detected PDCA-1^{+} cells in the lungs of infected wild-type (5% of total cells), as well as in the lungs (14%) and spleen (0.6%) of infected Ikaros$^{L/L}$ mice that were mostly lineage marker positive (CD19, CD3, Nk1.1. and CD11b), thus ruling out a mature pDC-population (data not shown).

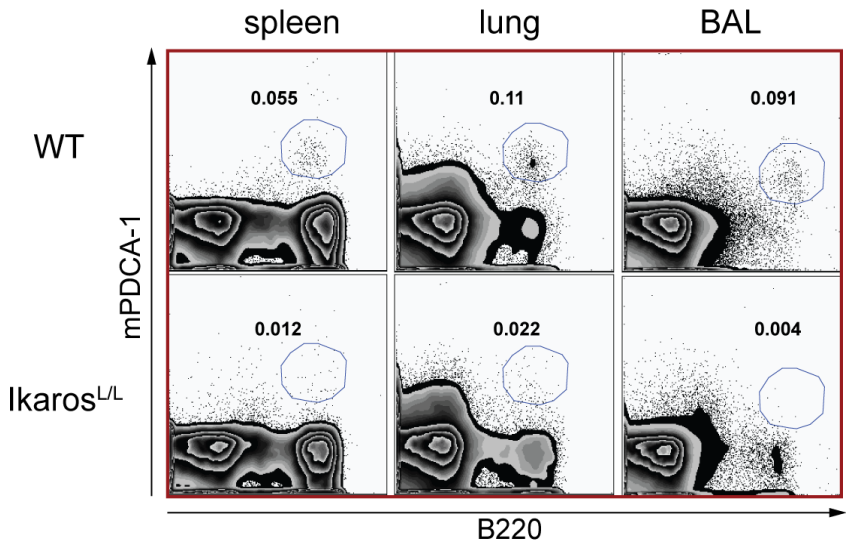

Figure 40: Mature pDCs are absent in Ikaros$^{L/L}$ mice during influenza virus infection.
Single cell suspensions of spleens, lungs and BAL of WT and Ikaros$^{L/L}$ mice were analyzed for the presence of B220^{+} mPDCA-1^{+} pDCs at day 10 post infection. Numbers depict percentage of pDCs per total cells in the respective organs. One of 2 independent experiments is shown.

Taken together, we concluded that pDCs are absent from peripheral and secondary lymphoid organs in Ikaros$^{L/L}$ mice both in the steady-state, and during influenza virus infection.

8.2.6. Ikaros$^{L/L}$ mice have impaired early T cell recruitment to the airways during influenza virus infection

Since pDCs can be a robust source of chemokines that act on effector cells such as T cells and NK cells [120, 123] (see chapter 1), we investigated whether Ikaros$^{L/L}$ mice have a defect in recruitment of these cells following infection with influenza PR8 virus.

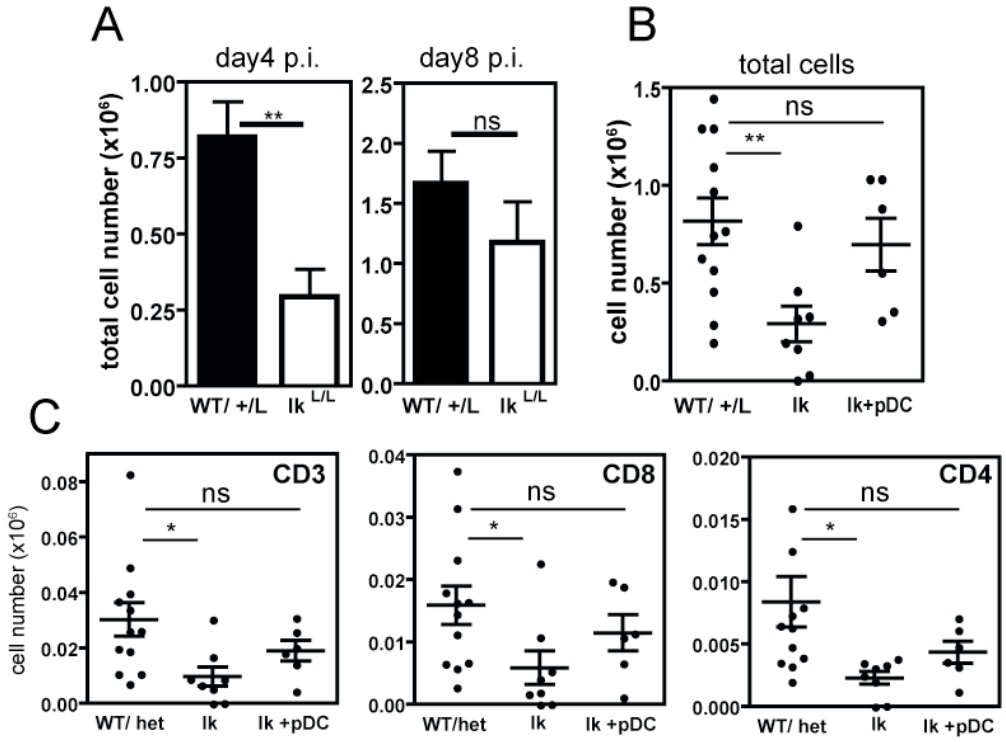

Figure 41: Absence of pDCs in Ikaros$^{L/L}$ mice results in delayed recruitment of T cells into the airways following influenza PR8 virus infection.

(**A**) Cells from the airways of infected WT (in some cases Ikaros$^{+/L}$ mice) or Ikaros$^{L/L}$ mice were collected by bronchioalveolar lavage (BAL). Total cell numbers were decreased in Ikaros$^{L/L}$ mice at day 4 p.i. (n=8-12mice, p=0.0048) but not significantly different at day 8 p.i. (n=7mice). (**B-C**) One day prior to infection, a group of Ikaros$^{L/L}$ mice was reconstituted with 2-3x10^6 pDCs intravenously. BAL was collected at day 4 and total cell numbers (**B**) and CD3$^+$ T cell subsets including CD8$^+$ and CD4$^+$ T cells (**C**) were enumerated.

We harvested cells in the bronchoalveolar space by lavage, and determined the numbers of immune cells at several time points post infection. As depicted in Figure 41A, BAL fluid of Ikaros$^{L/L}$ mice contained 3-fold lower total cell numbers compared to wild-type mice 4 days post infection. Particularly, CD8$^+$, CD4$^+$ T cells and NK cells were reduced, whereas the numbers of granulocytes were comparable to WT mice (data not shown). To confirm that this delay in recruitment was due to the absence of pDCs, we reconstituted Ikaros$^{L/L}$ mice with 2-3x10^6 pDCs one day prior to infection. Figure 41C-F shows that exogenous pDCs reversed the defect in cell recruitment, in particular that of T cells.

Together, we demonstrated that pDCs are important for the efficient recruitment of T cells into BAL early during influenza virus A infection, but not at later time points.

8.2.7. Activation of antigen-specific CD8$^+$ T cells and differentiation into effector T cells is normal in Ikaros$^{L/L}$ mice during PR8 infection

In order to rule out that the defect in T cell recruitment to the airways was due to impaired T cell activation, we investigated whether the CD8$^+$ T cell response in infected Ikaros$^{L/L}$ mice was comparable to WT mice. We made use of a modified PR8 virus expressing the LCMV glycoprotein epitope GP$_{33-41}$ (PR8-GP33), which are recognized by transgenic CD8$^+$ T cells from P14 mice. We adoptively transferred CFSE-labeled P14xThy1.1 cells into wild-type and Ikaros$^{L/L}$ mice to follow their proliferation. At day 4 p.i., we analyzed the cervical lymph nodes (cervLNs), which drain the upper respiratory tract including the nose. The transfer of cells from mice of the Thy1.1./Thy1.2 congenic background allows to distinguish Thy1.1 donor cells from endogenous Thy1.2 cells, so that transferred antigen-specific CD8$^+$ T cells can be easily tracked.

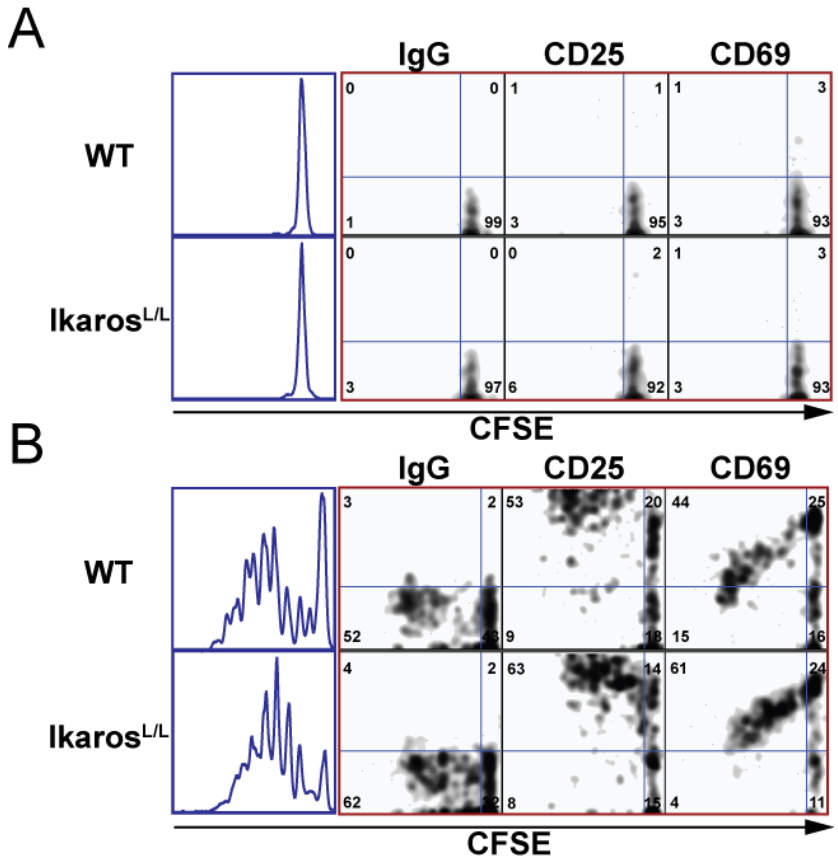

Figure 42: CD8⁺ T cell activation is normal in Ikaros$^{L/L}$ mice.

Splenocytes from P14xThy1.1 mice were labeled with CFSE and injected into WT and Ikaros$^{L/L}$ mice one day prior to infection with PR8-GP33. At day 4 p.i., transferred CD8⁺ T cells in cervLNs of uninfected control (**A**) and infected (**B**) mice were analyzed for proliferation and upregulation of the activation markers CD25 and CD69. Plots are gated on CD8⁺ Thy1.1⁺ cells.

CD8⁺ T cells in uninfected mice remained undivided and naïve as revealed by the absence of the activation markers CD25, CD69, and expression of high levels of L-selectin (Figure 42A and data not shown). However, in wild-type and Ikaros$^{L/L}$ mice infected with PR8-GP33, CD8⁺ P14 T cells had undergone multiple divisions at day 4 post infection. 80-90% of the antigen-specific cells showed an activated phenotype as they upregulated CD25 and temporarily also CD69 (Figure 42B). There was no difference in proliferation and activation of CD8⁺ T cells in WT and Ikaros$^{L/L}$ mice, suggesting that the absence of pDCs in

Ikaros$^{L/L}$ mice is not critical for priming and expansion of antigen-specific CD8$^+$ T cells following PR8 virus infection.

Next, we tested whether antigen-specific CD8$^+$ T cells activated in wild-type or Ikaros$^{L/L}$ mice acquire similar effector functions. To this end, we harvested spleens and lungs of animals at day 10 p.i., and assessed their ability to produce effector cytokines IFN-γ and TNF-α upon restimulation. A similar percentage of adoptively transferred CD8$^+$ T cells in the spleen and lungs of WT or Ikaros$^{L/L}$ mice produced IFN-γ and TNF-α upon restimulation (Figure 43 and data not shown).

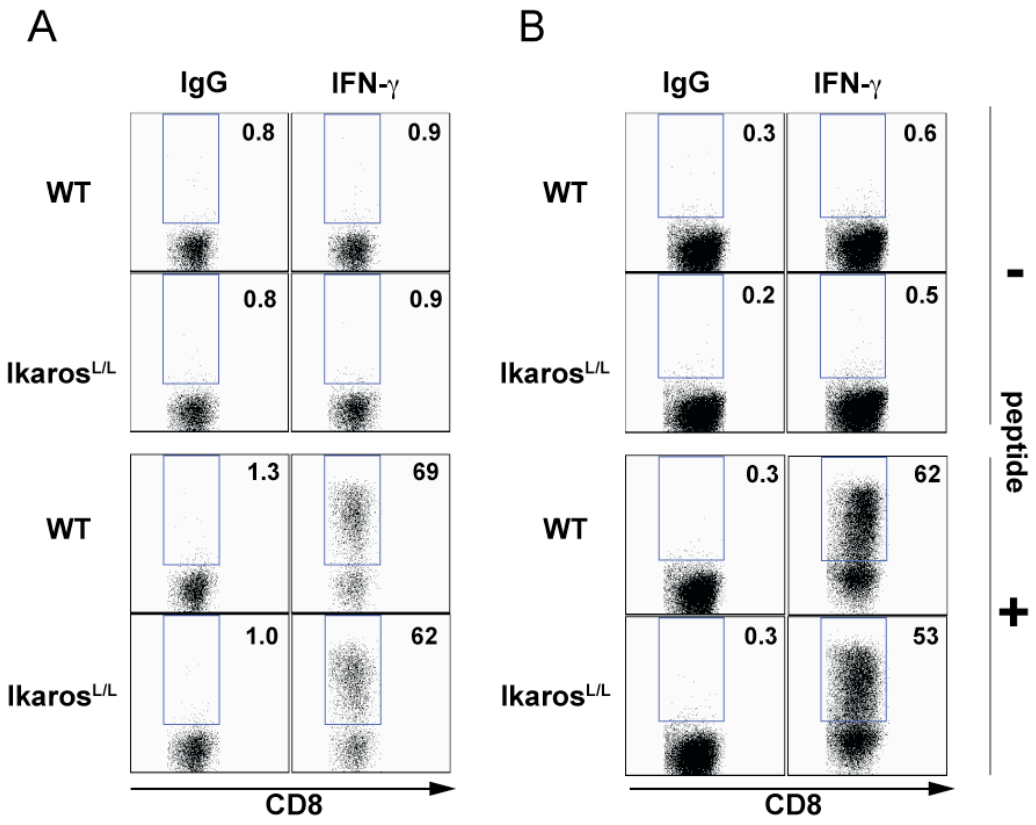

Figure 43: Effector functions of CD8$^+$ T cells in spleens and lungs of influenza virus infected WT and Ikaros$^{L/L}$ mice are comparable.

Spleens (**A**) and lungs (**B**) of WT and Ikaros$^{L/L}$ mice were harvested at day 10 p.i., and single cell suspensions were restimulated *in vitro* in the presence or absence of GP_{33-41} peptide (0.4 μg/ml) for 4 hours. Suspensions were stained with αCD8α and αThy1.1 and production of IFN-γ was assessed by intracellular cytokine staining.

8.2.8. Generation of memory CD8$^+$ T cells is normal in Ikaros$^{L/L}$ mice after PR8 infection

Since the precursor frequency of naïve antigen-specific T cells is artificially increased in the adoptive transfer model in comparison to the frequency of endogenous antigen-specific T cells, we assessed the generation of the endogenous antigen-specific memory CD8$^+$ T cells. This was made possible by the use of MHC class I tetramers that allow for tracking of CD8$^+$ T cells that recognize specific epitopes of the PR8 strain. One of the dominant CD8$^+$ T cell response in a primary infection is directed against the $NP_{366-374}$ of the viral nucleoprotein that is presented in context of $H2D^b$ [215].

When we analyzed circulating antigen-specific effector CD8$^+$ T cells in peripheral blood at day 8 p.i., we found a similar percentage of MHC tetramer$^+$ (Tet$^+$) cells in WT and Ikaros$^{L/L}$ mice (Figure 44A, left graph). Four weeks after infection, antigen-specific cells decreased in both WT and Ikaros$^{L/L}$ mice at comparable levels (Figure 44A, right graph). In the memory phase, it appeared that CD8$^+$ Tet$^+$ cells persisted to a similar extent in WT and Ikaros$^{L/L}$ mice in spleen (Figure 44B-D). In lungs, we found a trend towards higher percentages and total numbers of $D^bNP_{366-374}{}^+$ CD8$^+$ T cells in Ikaros$^{L/L}$ mice compared to WT mice, however the data were not statistically significant (Figure 44B and E-F).

In conclusion, we have shown that Ikaros$^{L/L}$ mice deficient in peripheral pDCs have normal CD8$^+$ T cell immune responses to a primary influenza virus infection.

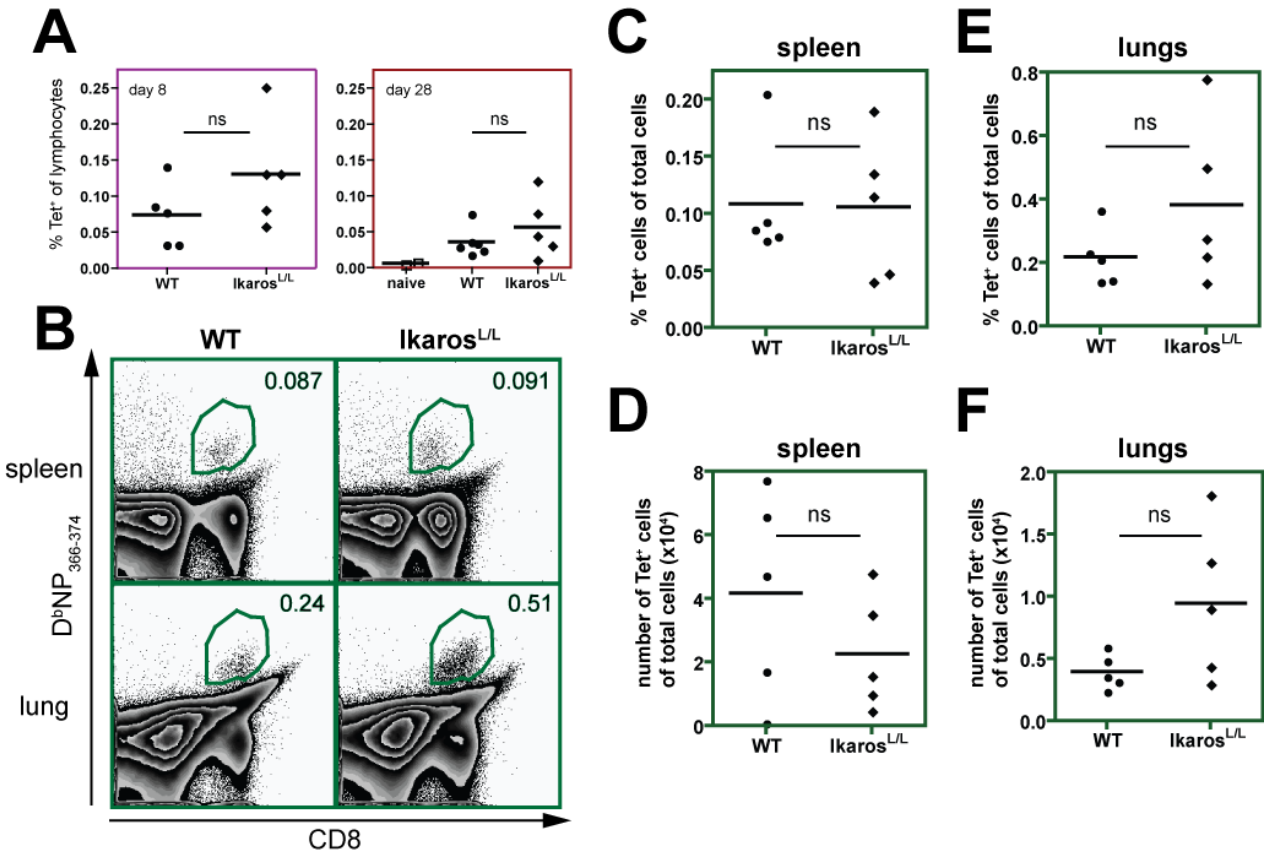

Figure 44: Formation of endogenous antigen-specific memory CD8$^+$ T cells is not impaired in Ikaros$^{L/L}$ mice following influenza virus infection.

(**A**) Peripheral blood was collected from naïve and infected WT and Ikaros$^{L/L}$ mice at day 8 and day 28 post infection. The percentage of D^{b}NP$_{366-374}$ tetramer$^+$ CD8$^+$ T cells was determined. (**B**) In the memory phase (day 39 p.i.), the percentage of tetramer$^+$ CD8$^+$ T cells in single cell suspensions of lungs and spleens of infected WT and Ikaros$^{L/L}$ mice was analyzed by flow cytometry. Percentages (**C, E**) and total numbers (**D, F**) of tetramer$^+$ CD8$^+$ T cells in spleens (**C, D**) and lungs (**E, F**) of infected WT and Ikaros$^{L/L}$ mice.

8.3. Discussion

In this chapter, we investigated the contributions of pDCs to anti-influenza immune response *in vivo*. Because pDCs are believed to play a central role in antiviral immunity due to their production of type I interferons, cytokines and chemokines (see Figure 6), we hypothesized that their functions are important for the resolution of infection.

We demonstrated that pDCs increase in numbers in the lungs and the airways during the response to influenza infection in WT mice (Figure 32), suggesting that they modulate the local environment during inflammation. To further analyze the precise role of pDCs during influenza infection, we made use of a mutant mouse strain, Ikaros$^{L/L}$, in which pDCs are absent in spleens, lungs and lymph nodes (Figure 34 and data not shown) [49]. To our surprise, we found no significant difference in morbidity of Ikaros$^{L/L}$ mice in response to intranasal infection of live influenza virus as compared to WT mice (Figure 37A). Moreover, Ikaros$^{L/L}$ mice recovered in a similar fashion with no significant prolonged increase in viral titers in the lungs (Figure 37B), suggesting that pDCs may not be crucial for the recovery of mice following influenza infection. These data are consistent with previous studies using mice that are unable to respond to type I interferons, i.e. IFNA-receptor knockout mice [216]. In these mice, viral titers in lungs were not significantly different from wild-type controls following infection with influenza PR8 virus. We demonstrated in chapter 1 that pDCs from IFNAR$^{-/-}$ mice remain immature following stimulation with PR8 virus. Interestingly, our results obtained with pDC-deficient mice resemble the findings in IFNAR$^{-/-}$ mice harboring pDCs that are unable to mature during PR8 infection. Furthermore, it was also shown that antibody titers from influenza A-infected IFNAR$^{-/-}$ mice were normal to elevated [216]. Although virus-activated pDCs have been implicated in inducing plasma cell differentiation and antibody production [97, 100], we observed comparable levels of influenza neutralizing antibodies in the serum of wild-type and Ikaros$^{L/L}$ mice despite slightly lower total B cell numbers (Figure 37 and data not shown) indicating that pDCs in this system are dispensable for B cell activation. It is possible that pDCs specifically target plasma cells [97] and thus

may become important in a secondary infection. Although we did not directly analyzed the $CD4^+$ T cell response, our results further suggest that $Ikaros^{L/L}$ mice have an undisturbed $CD4^+$ T cell helper response, which in turn can function normally to induce antibody-secretion of B cells.

In order to ascertain that pDCs are indeed dispensable for the resolution of influenza infection, we had to exclude that the $PDCA^+$ pDC-precursor present in the BM of $Ikaros^{L/L}$ mice exited into the periphery during inflammation. Although the precursor lacked some phenotypic and functional hallmarks associated with pDCs, i.e. they are $CD11c^-$, $B220^-$ and secreted only low amounts of IFN-α upon stimulation with virus (Figure 38), Allman et al. showed that these cells responded normally to Flt-3L treatment *in vitro* [49]. However, we found that after implantation of B16-Flt-3L cells the precursors in $Ikaros^{L/L}$ mice were unable to expand as well as pDCs in WT mice (Figure 39). Moreover, the precursors had a defect to mature not only after Flt-3L treatment (Figure 39), but also during influenza infection (Figure 40). Although we only tested the capacity of $Ikaros^{L/L}$ BM pDC-precursors to produce IFN-α, it is likely that other functions are impaired as well. Therefore, $Ikaros^{L/L}$ mice are indeed a good model to study disease in the absence of pDCs.

We observed that the lack of mature pDCs in $Ikaros^{L/L}$ mice resulted in reduced recruitment of cells into the bronchoalveolar space early upon infection, i.e. BAL of $Ikaros^{L/L}$ mice at day 4 p.i. contained 3-fold lower numbers of total cells compared to WT mice (Figure 41). The cell recruitment could be restored to normal levels when $Ikaros^{L/L}$ mice were reconstituted with pDCs prior to the infection (Figure 41). These results are the first to provide evidence that the influx of T cells into BAL following influenza virus infection is a pDC-dependent process. Due to the fact that pDCs are major producers of chemokines, such as CXCL9, CXCL10, CXCL11 and CCL4 [120, 123] (see also chapter 1), it seems likely that pDCs support the recruitment of $CXCR3^+$ and $CCR5^+$ cells to the lungs during infection. Our results are similar to the studies using $IFNAR^{-/-}$ mice that showed an impaired increase in numbers of virus-specific $CD8^+$ T effector cells into the airways up to day 6 following

infection with pneumonia virus and the X31 influenza virus strain [216, 217]. The comparable number of cells in BAL at day 8 p.i. suggests that compensatory mechanisms come into play that can overcome the defect of chemokine production in the absence of pDCs. It has been shown that upon depletion of pDCs, other cells could be induced to produce higher levels of cytokines such as IL-12 to compensate for a lack of function of pDCs during MCMV infection [46]. The same mechanism of compensation could be envisioned for chemokines.

We performed experiments to exclude the possibility that the lack of T cell recruitment into BAL is due to a dysfunction during effector T cell differentiation. We transferred CFSE-labeled T cells specific for the LCMV peptide GP_{33-41} into wild-type and $Ikaros^{L/L}$ mice. Following infection with recombinant virus PR8-GP33, we observed that antigen-specific donor cells proliferated equally well in both recipient mouse strains (Figure 42). Similar levels of activation markers and IFN-γ suggest that $CD8^+$ T cell differentiation was not impaired in the absence of pDCs (Figure 43). These results are consistent with previous studies, which have shown that pDCs are not the major antigen presenting cells following influenza virus infection [108, 109]. In these studies, pDCs from mice infected with a recombinant influenza virus did not induce antigen-specific T cell proliferation. Furthermore, we found that pDCs did not accumulate in the lung-draining medLNs and did not upregulate costimulatory molecules in contrast to myeloid dendritic cells ($CD11c^{hi}$ cells), which rapidly increased in numbers between 24 h and 72 h post infection (Figure 32E-F and data not shown). It has previously been shown that this is the time window when the primary antigen presentation to T cells occurs [20, 109]. A recent study using HSV infection as a model also indicated that pDCs act on mDCs to provide help for their antigen presenting capacity [174]. However, we showed *in vitro* and *in vivo* that the lack of pDCs was not significantly influencing the maturation of DCs, by demonstrating that DCs and B cells can respond normally to viral activation (Figure 36 and data not shown). Consistent with these results, published data have shown that the levels of IL-12, which is mainly produced by macrophages and DCs, following injection of various Toll-like receptor ligands was unaltered in $Ikaros^{L/L}$ mice [49]. Taken together, these data in addition to the results presented

in chapter one allow us to conclude that pDCs activated by influenza virus may not be involved in class I-restricted antigen presentation in a primary immune response to influenza virus infection.

However, type I interferons are thought to act and promote $CD8^+$ T cell cross-priming and differentiation as a stimulatory co-factor [88]. Neither in IFNAR-knockout mice [216] nor in $Ikaros^{L/L}$ mice did effector $CD8^+$ T cells have diminished or altered cytokine production. In addition, the formation of memory T cells specific for the $NP_{366-374}$ peptide of PR8 virus appeared to be normal in the lungs and spleens of $Ikaros^{L/L}$ mice (Figure 44). These results suggest that pDCs and their functions may not be essential for $CD8^+$ T cell responses following a primary influenza virus infection and that pDCs are dispensable for clearance of PR8 virus. Although we had hypothesized that mice may be unable to clear the virus in the absence of pDCs, we found no evidence that influenza virus persisted in $Ikaros^{L/L}$ mice as mentioned above. In case of a persistent viral infection, we also would expect to find an impaired T cell compartment, as persistence is often associated with a dysfunctional or suppressed T cell responses induced by a wide range of viruses including HIV, CMV, EBV and hepatitis infection [218]. Our results, however, demonstrate that the numbers (Figure 44), the phenotype, and the functional capacities (data not shown) of memory $CD8^+$ T cells are not impaired in $Ikaros^{L/L}$ mice.

Although we did not directly address the possibility that PR8 virus may have disseminated to other organs besides the lungs during infection, a previous study in PR8-infected IFNAR-deficient mice demonstrated that no extrapulmonary viral antigens could be found. Interestingly, another group infected IFNAR-deficient mice with the influenza virus strain A/WSN33 [219], and could show that the virus disseminated to other organs including the spleen, liver and brain of these mice. The WSN strain, however, has an atypical virulence behavior as it is able to sequester plasminogen and thus provides enhanced HA cleavage, which results in greater virulence [220]. Type I interferon may thus be very important to restrict viral replication to the lungs in specifically virulent infections, which may therefore

require pDCs. The study presented here does not exclude the possibility that the role of pDC-derived type I interferon, and presumably other pDC functions, may become important in the defense against more virulent strains or a systemic viral infection rather than a localized disease. Thus, two studies using a model of murine respiratory syncytial virus infection showed that pDC depletion resulted in increased pulmonary pathology, and that adoptive transfer of pDCs promoted viral clearance [172, 173]. However, depletion with the 120G8 antibody potentially decreases other cell subsets that may contribute to the resolution of infection. To demonstrate that pDCs can enhance viral elimination, Wang et al. activated bone marrow-derived pDCs with CpG 1826 prior to intratracheal transfer into animals that were subsequently infected with RSV. As shown in chapter one, pDCs activated with CpG 1826 acquire functions and express cytokines different from pDCs activated by virus, thus this approach may not resemble the functions of RSV-stimulated pDCs *in vivo*.

In summary, we have demonstrated that pDC functions during a primary immune response to influenza virus infection are limited to the recruitment of T cells into the bronchioalveolar space. PDCs appear to be dispensable for the clearance of virus, antigen presentation, priming and differentiation into effector/memory $CD8^+$ T cells as well as the production of virus-neutralizing antibodies. Thus, the results of this study imply that pDCs may be dispensable for the recovery from a primary infection with influenza PR8 virus.